Received: 15 January 2020 | Revised: 21 May 2020 | Accepted: 8 June 2020

DOI: 10.1002/aoc.5906

FULL PAPER

Applied Organometallic Chemistry WILEY

MWCNTs-ZrO_2 as a reusable heterogeneous catalyst for the synthesis of *N*-heterocyclic scaffolds under green reaction medium

Bipasa Halder | **Flora Banerjee** | **Ahindra Nag**

Department of Chemistry, Indian Institute of Technology Kharagpur, Kharagpur, 721302, India

Correspondence
Ahindra Nag, Department of Chemistry, Indian Institute of Technology Kharagpur, Kharagpur 721302, India.
Email: ahinnag@chem.iitkgp.ernet.in

Funding information
UGC, NEW DELHI, INDIA, Grant/Award Number: Ref No.- 21/06/2015(i)EU-V

A simple, efficient, and facile heterogeneous multi-walled carbon nanotubes-zirconia nanocomposite (MWCNTs-ZrO_2) has been synthesized using natural feedstock coconut juice (água-de-coco do Ceará). The synthesized catalyst was characterized by Fourier transform infrared spectroscopy, X-ray diffraction, field emission scanning electron microscopy, and X-ray photoelectron spectroscopy analysis. The heterogeneous nanocomposite has been used for one-pot synthesis of various *N*-heterocyclic compounds like pyrazoles, 1,2-disubstituted benzimidazoles, 2-arylbenzazoles, and 2,3-dihydroquinazolin-4(1*H*)-ones under green reaction medium at room temperature. This novel method has several advantages, such as short reaction time, simple work-up, excellent yield, and green reaction conditions. The catalyst was recycled up to four times without significant loss in catalytic activity.

KEYWORDS

coconut juice, heterogeneous catalyst, MWCNTs-ZrO_2, *N*-heterocyclic compounds, one-pot synthesis

1 | INTRODUCTION

Nitrogen-containing heterocyclic (azaheterocyclic) privileged scaffolds are widely dispersed in diverse fields such as synthetic organic chemistry, pivotal intermediates in drug industry, and biological and pharmaceutical areas.[1] Many pyrazole derivatives in synthetic chemistry, and amino pyrazoles are fascinating due their numerous properties, for example antifungal,[2] antimicrobial,[3] antiviral,[4] antihyperglycemic,[5] antitumor,[6] anti-inflammatory,[7] analgesic,[8] antidepressant,[9] and anti-convulsant.[10] Of the many reported methods, most of the conventional approaches for the synthesis of pyrazoles are multicomponent reactions (MCRs) between a variety of aldehydes, malononitrile, and phenylhydrazine, which are synthesized using different types of catalyst, such as I_2,[11] GO-TiO_2,[12] polyethylene glycol:H_2O,[13] CuO/ZrO_2,[14] {[HMIM]$C(NO_2)_3$},[15] Fe_3O_4@Si@MoO_2,[16] and CPS-CDMNPs.[17]

Benzimidazole derivatives are fused *N*-heterocyclic skeletons that possess different biological properties such as anti-inflammatory,[18] antiprotozoal,[19] antihelminthic,[20] antimicrobial,[21] and anticancer activities,[22] 5-lipoxy genase inhibitory activities,[23] and antihypertensive activities.[24] Recently, several methods have emerged for the synthesis of 1,2-disubstituted benzimidazole derivatives in the presence of various catalysts such as ionic liquid-coated ZnO nanoparticles,[25] chitosan-supported Fe_3O_4,[26] Zn-proline,[27] and trifluoroethanol,[28] as well as benzimidazole derivatives synthesized from sodium dodecyl sulfate micelles,[29] $Er(OTf)_3$,[30] and graphene sulfonic acid[31] catalysts. In addition, benzothiazole motifs are of outstanding significance due to their anticancer, antitumor, and antibacterial activities.[29] Several methodologies have

been disclosed for the synthesis of benzothiazoles, such as SDS micelles,[29] nano-Fe_2O_3,[32] Bu^{t}ONa,[33] and oxalic/malonic acid.[34]

2,3-dihydroquinazolin-4(1*H*)-ones (DHQs) are *N*-hetero bicyclic compounds that have wide-ranging application as drug intermediates in the pharmaceutical and biological fields.[35] A number of methods have been established for the synthesis of DHQs over silica sulfuric acid,[36] beta cyclodextrin,[37] PEG-400,[35] Co-CNTs,[38] montmorillonite K-10,[39] and $[Ce(L\text{-}Pro)_2]_2(Oxa)$.[40]

Heterogeneous catalysis is widely used and has become important for organic transformations in recent years.[41] Heterogeneous catalysts have many advantages over homogeneous catalysts, such as simple work-up, easy handling, reusability, and recoverability.[42] Notably, carbon nanotubes (CNTs) have attracted much attention in the field of heterogeneous catalysis[43] due to their high surface area, unique morphology, network, physical properties, and high electrical conductivity.[44] Recently, carbon nanotubes and their composites have been used as catalysts in many organic reactions as well as in the pharmaceutical industry.[38,45]

Among the various ceramic oxide nanoparticles, ZrO_2 has been used as a heterogeneous catalyst because of its high dielectric properties and thermal stability, acid–base properties and good mechanical strength.[46] Likewise, it has many applications in the field of science and technology.[47] Therefore multi-walled CNTs-ZrO_2 (MWCNTs-ZrO_2) composites have been used in the field of Electromagnetic interference shielding.[48] Hybridization of MWCNTs-ZrO_2 composites has not been used in organic synthesis as a heterogeneous catalyst till now.

From the perspective of green chemistry, water has attracted attention as a reaction medium due to its cheap, environmentally friendly, nontoxic, and nonflammable properties.[49] Recently, plant parts have been used as a biocatalyst for organic transformations and generating nanoparticles also due to its mild reaction condition and eco-friendly aqueous medium.[50] In this context, coconut juice was introduced to the field of green nanotechnology. Coconut juice, known as água-de-coco do Ceará (ACC), is a sweet refreshing juice. Each 100 g of coconut juice contains water (94.99 g), proteins (0.72 g), fat (0.2 g), carbohydrates (3.71 g), fiber (1.1 g), sugar (2.61 g), electrolytes such as sodium (105 mg) and potassium (250 mg), minerals such as calcium (24 mg), magnesium (25 mg), and phosphorous (20 mg), ascorbic acid (2.4 mg), and pantothenic acid (0.043 mg).[51] It is already known that many fruit extracts, which are acidic in nature, have been used to synthesize ZrO_2 nanoparticles.[52] We report here the first synthesis of ZrO_2 and MWCNTs-ZrO_2 nanoparticles using ACC. Due to the acidic nature of ACC (pH = 5.06), it accelerates the formation of MWCNTs-ZrO_2 nanocomposite.

We describe the synthesis of MWCNTs-ZrO_2 nanocomposite from ACC and demonstrate its application as an efficient heterogeneous catalyst for the synthesis of pyrazoles by a multicomponent reaction of phenylhydrazine, malononitrile, aldehydes, synthesis of 1,2-disubstituted benzimidazoles and benzimidazoles from *o*-phenylenediamine and benzaldehydes, synthesis of benzothiazoles from *o*-aminothiophenol and benzaldehydes, and synthesis of 2,3-dihydroquinazolin-4(1*H*)-ones from 2-aminobenzamide and benzaldehydes at room temperature (Scheme 1).

2 | RESULTS AND DISCUSSION

2.1 | Characterizations of the synthesized nanocomposite

ZrO_2 and MWCNTs-ZrO_2 were synthesized using a simple refluxing method from the natural feedstock ACC. The bonding, crystallinity, morphology, and atomic composition of the product were examined by Fourier transform infrared (FT-IR) spectroscopy, X-ray diffraction (XRD), field emission scanning electron microscopy (FE-SEM), and X-ray photoelectron spectroscopy (XPS), respectively.

The FT-IR spectra of oxidized MWCNT, ZrO_2, and MWCNTs-ZrO_2 composite were recorded in the range of 4,000–400 cm^{-1} and the findings are displayed in Figure 1. The prominent peaks in spectra of oxidized MWCNT and ZrO_2 at ~1,222 and 769 cm^{-1} correspond to C–O bond stretching in different chemical environments and C–H bending vibration, respectively.[53] The two peaks in the spectra of ZrO_2 can be attributed to some metabolite and protein, such as the flavonoids and terpernoids present in coconut juice.[50f] Broad peaks centered at ~3,360, 1,611, and 1,349 cm^{-1} appeared in the ZrO_2 spectrum due to the stretching and bending modes of the –OH group originating from adsorbed moisture.[53c,54] Notably, the weak and broad peak centered at ~968 cm^{-1} is related to the Zr–O stretching mode. The FT-IR spectrum of the MWCNTs-ZrO_2 composite exhibited superimposition of the spectral features of both oxidized MWCNTs and ZrO_2, accompanied by a change in peak intensity. Weak peaks centered at ~1,120 and 1,017 cm^{-1} appeared in the spectrum for the MWCNTs-ZrO_2 composite due to the stretching mode of the aromatic C=C and C–O groups, respectively, presenting different chemical environment.[48] These findings clearly signify successful incorporation of ZrO_2 into MWCNTs.

SCHEME 1 Synthesis of *N*-heterocyclic scaffolds in the presence of MWCNTs-ZrO_2

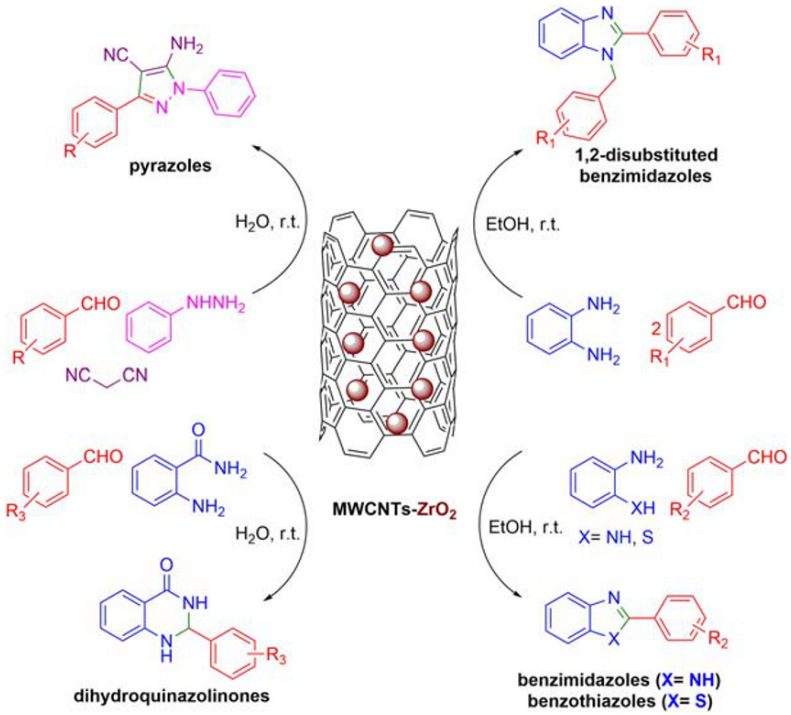

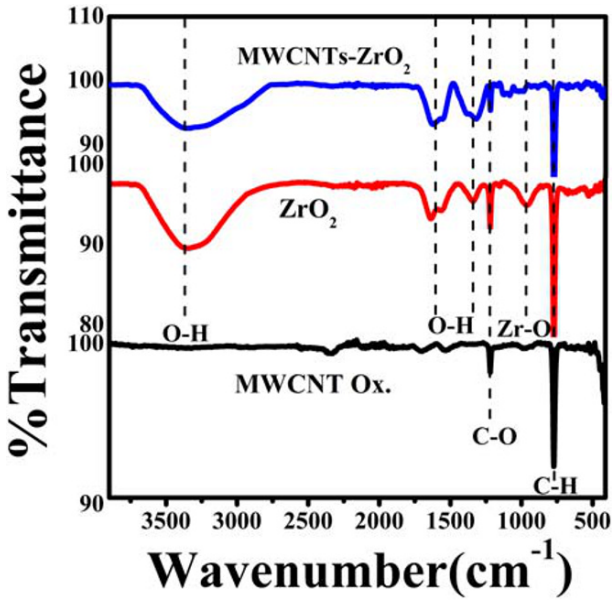

FIGURE 1 FT-IR spectra of oxidized MWCNTs, ZrO_2, and MWCNTs-ZrO_2 composite

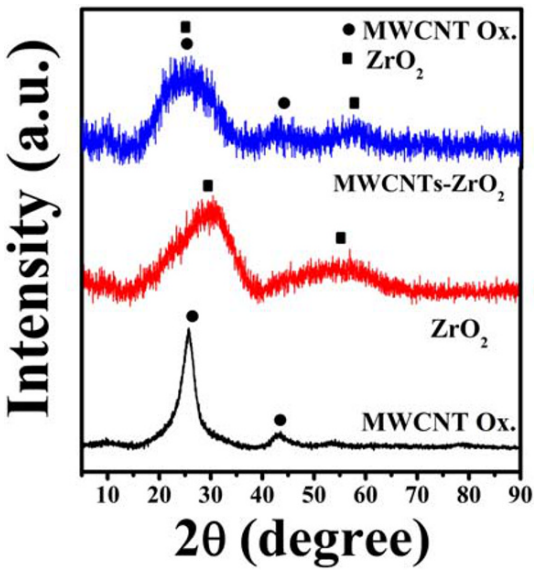

FIGURE 2 XRD pattern of oxidized MWCNTs, ZrO_2, and MWCNTs-ZrO_2 composite

XRD patterns of oxidized MWCNTs, ZrO_2, and MWCNTs-ZrO_2 composites are shown in Figure 2. It can be seen that diffraction peaks for oxidized MWCNTs occur at $2\theta = \sim 26^\circ$ and $\sim 43^\circ$, corresponding to the (002) and (100) planes, respectively, of MWCNTs.[55] Furthermore, the appearance of two broad peaks centered at around $\sim 30^\circ$ (002) and 55° (100) confirmed the formation of amorphous from ZrO_2 (JCPDS no. 37–1,484).[56] XRD patterns for the MWCNTs-ZrO_2 composite had diffraction peaks for both ZrO_2 and oxidized MWCNTs. Notably, the breadth of the oxidized MWCNT peak centered at $\sim 26^\circ$ increased and the peak intensity of the same peak decreased with incorporation of amorphous ZrO_2 in MWCNTs. These findings clearly indicate incorporation of ZrO_2 into the MWCNT matrix.

FE-SEM images of ZrO_2, oxidized MWCNTs, and MWCNTs-ZrO_2 composite are shown in Figure 3. ZrO_2 appears to exist as agglomerated spherical nanoparticles.[48]

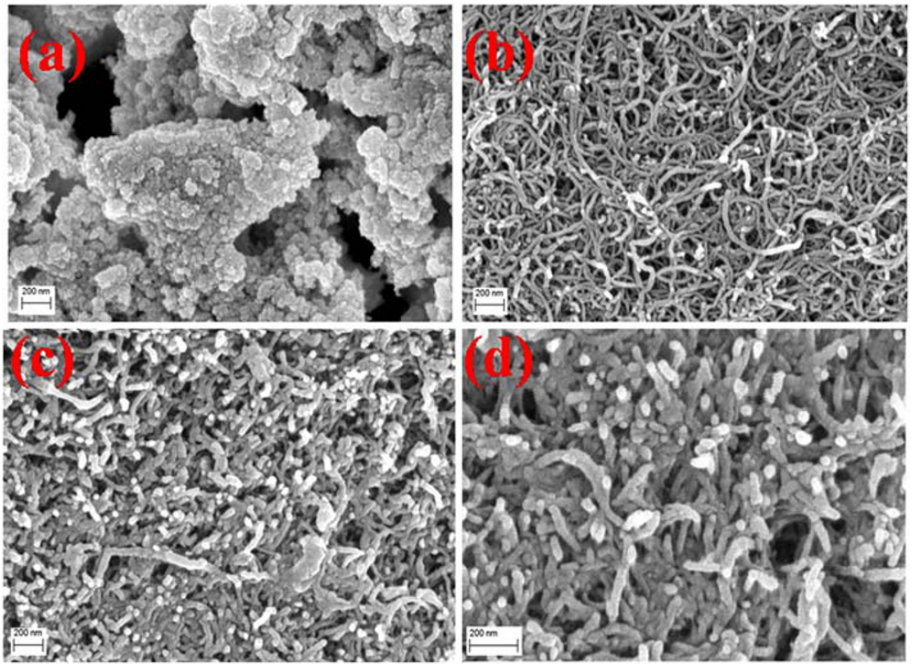

FIGURE 3 FE-SEM images of (a) ZrO_2, (b) oxidized MWCNT, and (c) low-magnification and (d) high-magnification images of MWCNTs-ZrO_2 composite

Oxidized MWCNTs exhibit nanotube-like morphology stacked together. FE-SEM images of MWCNTs-ZrO_2 composite show that ZrO_2 nanoparticles are clearly incorporated in the MWCNT matrix. Notably, the regular shape of the MWCNTs remains intact even after synthesis with ZrO_2.[48]

The valence state and elemental analysis of MWCNTs-ZrO_2 composite were analyzed by XPS (Figure 4). Figure 4a shows the full survey spectrum of the MWCNTs-ZrO_2 composite, which confirms the presence of C, O, and Zr elements. Figure 4b shows deconvoluated peaks for the Zr 3d spectrum at 183.7 and 186.2 eV, corresponding to Zr $3d_{3/2}$ and Zr $3d_{5/2}$, respectively.[57a] Deconvoluated peaks at 284.9, 286.3, and 288.2 eV in the high-resolution C 1 s spectrum are associated with the C–C, C–O, and C=O functionalities, respectively.[57a] The fine spectrum of O 1 s in the as-prepared composite reveals peaks at 531.3, 532.4, and 533.5 eV, corresponding to Zr–O, C=O, and O–C=O, respectively.[57] All these findings point to the oxidized nature of MWCNTs and the presence of ZrO_2 in the MWCNTs-ZrO_2 composite.

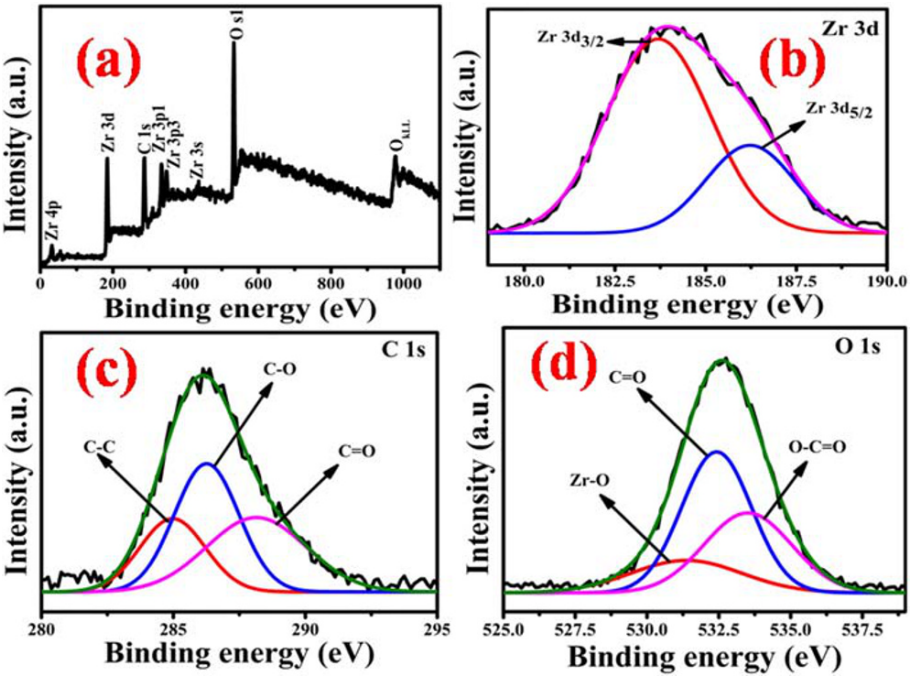

FIGURE 4 XPS spectra of MWCNTs-ZrO_2 composite: (a) full survey spectra, (b) Zr 3d, (c) C 1 s, and (d) O 1 s

2.2 | One-pot synthesis of pyrazole derivatives

The catalytic activity of MWCNTs-ZrO_2 was examined for the multicomponent reaction of substituted benzaldehydes, phenyl hydrazine, and malononitrile (Scheme 2). To optimize the suitable reaction conditions for the synthesis of pyrazole derivatives, *p*-nitro benzaldehyde (1 mmol), phenyl hydrazine (1 mmol), and malononitrile (1 mmol) were chosen as model reactants in the presence of MWCNTs-ZrO_2 nanocomposite and the results are summarized in Table 1. When the reaction was carried out in the absence of a catalyst, no product was formed after 10 hr at room temperature or at high temperature (Table 1, entries 1 and 2). The same reaction was performed in the presence of MWCNT (10 mg) and ZrO_2 (10 mg) in water (5 ml) as solvent at room temperature, giving the products in yields of 35% and 40%, respectively (Table 1, entries 3 and 4).

When the reaction was carried out in the presence of MWCNTs-ZrO_2 catalyst (10 mg), the yield of the product was 92% in water at room temperature (Table 1, entry 5). Solvents with different polarities, such as EtOH, MeOH, dichloromethane (DCM), MeCN, and H_2O, were used to determine the best solvent and H_2O was found to be the best reaction medium for the synthesis of pyrazole (Table 1, entries 1–11). It is noteworthy that there was no significant improvement in the yield of product on increasing the amount of catalyst from 10 mg to 20 mg (Table 1, entries 5 and 6). Further increasing the temperature had no effect on the yield of the desired product (Table 1, entry 11). After optimization of the reaction conditions, the scope of the reaction was extended by using different aromatic aldehydes, phenylhydrazine, and malononitrile to obtain the products **4a–p**, which are summarized in Figure 5. In all cases, aromatic aldehydes containing electron-withdrawing as well as electron-donating compounds showed good to excellent yield. The structures of all products were characterized by FT-IR, ^{1}H NMR, and ^{13}C NMR spectroscopy analysis.

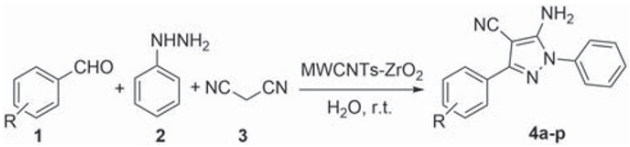

SCHEME 2 Synthesis of pyrazole derivatives **4**

2.3 | One-pot synthesis of 1,2-disubstituted benzimidazole derivatives

As a result of the success of the synthesis of pyrazole reactions, the utility of the nanocomposite MWCNTs-ZrO_2 was extended to the synthesis of 1,2-disubstituted

TABLE 1 Optimization of the reaction conditions for the synthesis of pyrazole **4a**[a]

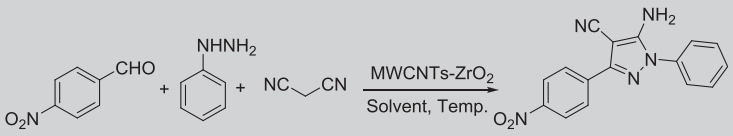

Entry	Catalyst (mg)	Solvent	Temperature (°C)	Time (hr)	Yield (%)[b]
1	–	H_2O	r.t.	10	–
2	–	H_2O	60	10	–
3	MWCNT (10)	H_2O	r.t.	5	35
4	ZrO_2 (10)	H_2O	r.t.	5	40
5	**MWCNTs-ZrO_2 (10)**	**H_2O**	**r.t.**	**1.5**	**92**
6	MWCNTs-ZrO_2 (20)	H_2O	r.t.	1.5	92
7	MWCNTs-ZrO_2 (10)	EtOH	r.t.	1.5	88
8	MWCNTs-ZrO_2 (10)	MeCN	r.t.	1.5	78
9	MWCNTs-ZrO_2 (10)	DCM	r.t.	1.5	82
10	MWCNTs-ZrO_2 (10)	MeOH	r.t.	1.5	85
11	MWCNTs-ZrO_2 (10)	H_2O	60	1.5	92

[a]Reaction conditions: *p*-nitro benzaldehyde (1 mmol), phenylhydrazine (1 mmol), malononitrile (1 mmol), and MWCNTs-ZrO_2 nanocomposite in solvent (5 ml).
[b]Isolated yield.

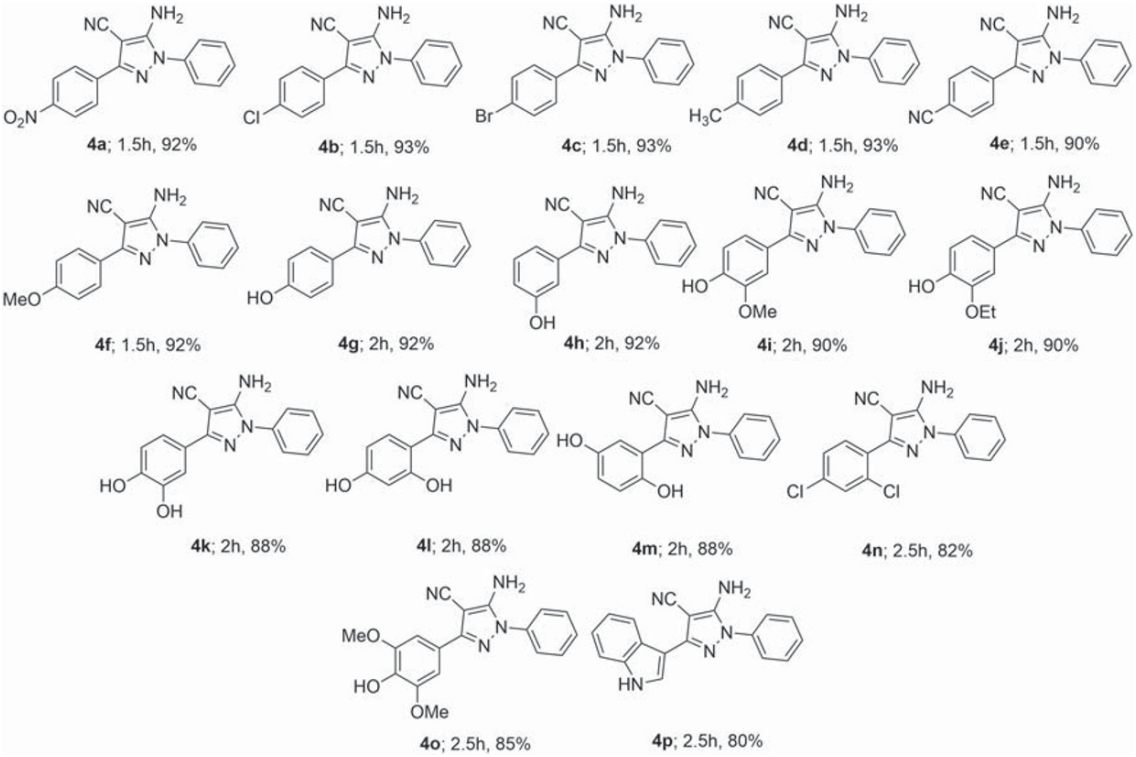

FIGURE 5 Synthesis of pyrazole derivatives in the presence of MWCNTs-ZrO_2 nanocomposite

benzimidazole by cyclocondensation of 1 mol of *o*-phenylenediamine and 2 mol of various benzaldehydes (Scheme 3).

At the outset of the present study and to optimize the reaction conditions for the synthesis of disubstituted benzimidazole derivatives, *o*-phenylenediamine (1 mmol) and *p*-hydroxybenzaldehyde (2 mmol) in the presence of MWCNTs-ZrO_2 nanocomposite with different solvents were chosen as a model reaction and the results are summarized in Table 2.

The cyclocondensations of *o*-phenylenediamine (1 mmol) and various aromatic benzaldehydes (2 mmol) with MWCNTs-ZrO_2 nanocomposite in EtOH under optimized reaction conditions are summarized in Figure 6. In all cases, aromatic aldehydes containing electron-withdrawing as well as electron-donating compounds showed good to excellent yield. The structures of the products **7a–o** were characterized by FT-IR, ^{1}H NMR, and ^{13}C NMR spectroscopy analysis.

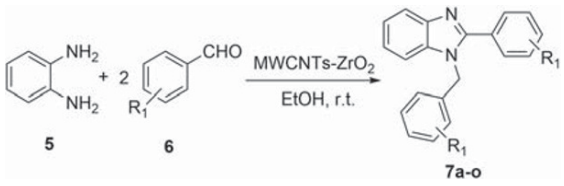

SCHEME 3 Synthesis of 1,2-disubstituted benzimidazole derivatives **7**

2.4 | One-pot synthesis of 2-arylbenzazole derivatives

The outlook of *o*-substituted aniline system has been continued for the synthesis of 2-aryl benzimidazole and 2-aryl benzothiazole derivatives (Scheme 4) under the same reaction conditions as shown in Table 2 (entry 8).

For the synthesis of 2-aryl benzimidazole derivatives, *o*-phenylenediamine (1 mmol) and various aromatic benzaldehydes (1 mmol) with MWCNTs-ZrO_2 nanocomposite were stirred in EtOH. For the synthesis of 2-aryl benzothiazole derivatives, 2-aminothiophenol (1 mmol) was used instead of *o*-phenylenediamine with various aromatic aldehydes (1 mmol) and MWCNTs-ZrO_2 nanocomposite (10 mg) in EtOH. All compounds **9a–j** are summarized in Figure 7. From Figure 7, it is concluded that aromatic aldehydes containing electron-donating as well as electron-withdrawing compounds showed good to excellent yield. The structures of all products were characterized by FT-IR, ^{1}H NMR, and ^{13}C NMR spectroscopy analysis.

2.5 | One-pot synthesis of dihydroquinazolinone derivatives

The catalytic activity of MWCNTs-ZrO_2 was investigated for the synthesis of dihydroquinazolinone derivatives,

TABLE 2 Optimization of the reaction conditions for the synthesis of disubstituted benzimidazole **7b**[a]

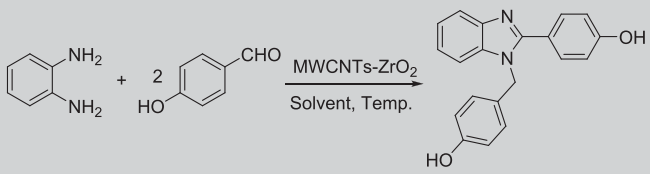

Entry	Solvent/catalyst	Temperature (°C)	Time (hr)	Yield (%)[b]
1	H_2O/10 mg	r.t.	2	40
2	H_2O/20 mg	r.t.	2	45
3	MeCN/10 mg	r.t.	2	50
4	DCM/10 mg	r.t.	2.5	60
5	$CHCl_3$/10 mg	r.t.	2.5	62
6	MeOH/10 mg	r.t.	2	75
7	EtOH/10 mg	r.t.	2	85
8	**EtOH/10 mg**	**r.t.**	**3**	**92**
9	EtOH/20 mg	60	3	92

Bold emphasis highlight the optimal reaction conditions giving excellent yield.

[a]Reaction conditions: *o*-phenylenediamine (1 mmol), *p*-hydroxybenzaldehyde (2 mmol), and MWCNTs-ZrO_2 nanocomposite in solvent (5 ml).

[b]Isolated yield.

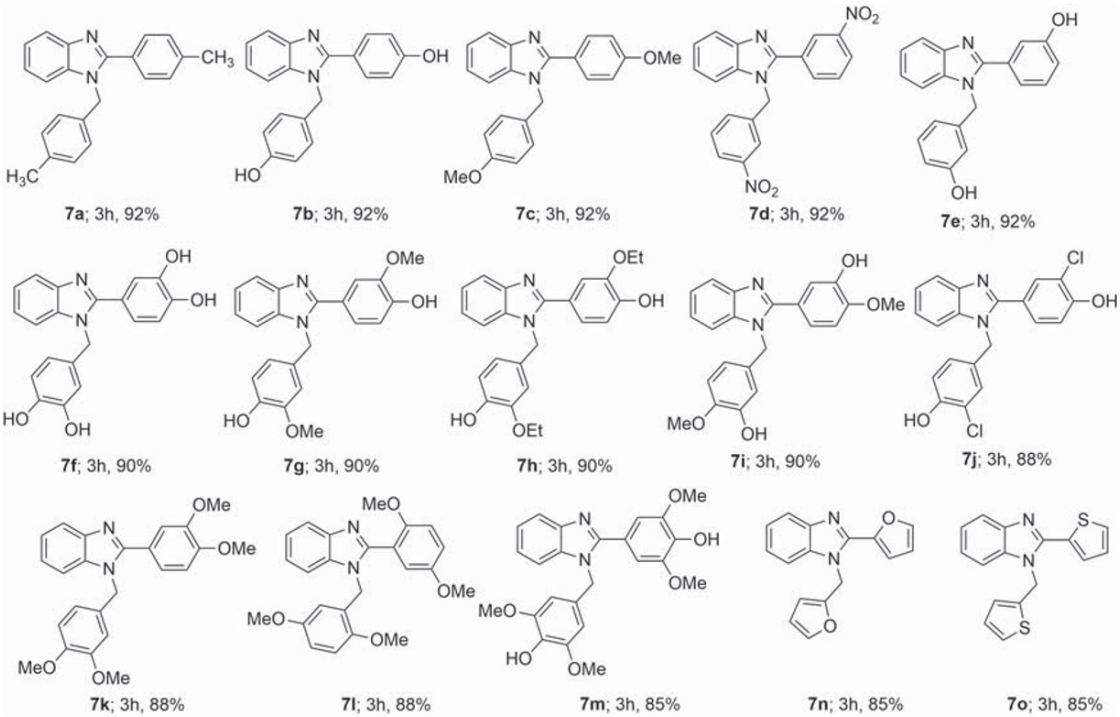

FIGURE 6 Synthesis of 1,2-disubstituted benzimidazole derivatives in the presence of MWCNTs-ZrO_2 nanocomposite

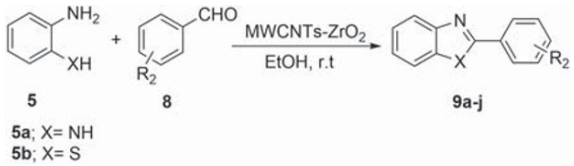

SCHEME 4 Synthesis of 2-arylbenzazole derivatives **9**

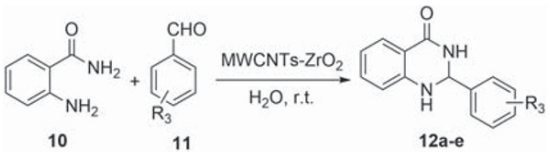

SCHEME 5 Synthesis of dihydroquinazolinone derivatives **12**

keeping water as a solvent at room temperature (Scheme 5).

To optimize the reaction conditions, the reaction between 2-aminobenzamide (1 mmol) and 4-hydroxy-3,5-dimethoxy benzaldehyde (1 mmol) was used as a model reaction in the presence of MWCNTs-ZrO_2 nanocomposite and the results are summarized in Table 3.

The products obtained from the condensation of 2-aminobenzamide (1 mmol) and various aromatic benzaldehydes (1 mmol) with MWCNTs-ZrO_2 nanocomposite in H_2O under optimal conditions are summarized in Figure 8 and have moderately good yield. The structures of compounds **12a–e** were characterized by FT-IR, ^{1}H NMR, and ^{13}C NMR spectroscopy analysis.

To demonstrate the efficiency of the present protocol, the results obtained for the synthesis of compounds **4f**, **7b**, **9h**, and **12b** were compared with some previous reported methods (Table 4). From Table 4, it is clear that the present system is comparable with reported procedures with respect to solvent and yields.

Catalyst reusability was screened for the synthesis of products **4f**, **7b**, **9h**, and **12b**. For compounds **4f** and **12b** the catalyst was recovered from the aqueous part of the reaction mixture after work-up with ethyl acetate. The catalyst was washed with EtOH and DCM several times, then dried in an oven at 60°C. For compounds **7b** and **9h**, the reaction mixtures were evaporated under reduced pressure to remove EtOH. The residues were extracted after a conventional work-up with ethyl acetate and water, and the catalyst was recovered by above stated procedure. In this way, the catalyst was recovered four times and a slight loss of catalytic activity was observed for each reaction. The results are shown in Figure 9.

3 | EXPERIMENTAL

3.1 | Materials and characterization

All reagents were purchased from Merck, Sigma-Aldrich, and Fluka, Bangalore. The reactions were monitored using precoated aluminum TLC plates (Mark silica 60, f_{254}). XRD measurements were recorded at room temperature to characterize MWCNTs, oxidized MWCNTs, and MWCNTs-ZrO_2 using a Phillip, Holland, Bangalore instrument with CuKα radiation at $\lambda = 0.1541$ nm. The morphology of the samples was studied by FE-SEM on a Carl Zeiss, Bangalore at an accelerating voltage of 20 kV. XPS of the nanocomposite was examined using a PHI 5000 Versa Probe II system, Bangalore using a microfocused (100 μm, 25 W, 15 kV) monochromatic Al Kα source ($h\nu = 1486.6$ eV). NMR spectra were recorded on a Bruker Avance, Bangalore 400 MHz, 500 MHz or 600 MHz spectrometer using DMSO-d_6 or $CDCl_3$ as the solvent. The multiplicity was marked as s (singlet), d (doublet), t (triplet), m (multiplet), and or (broad singlet). Melting points were determined in open capillary using an Electrothermal 9,100, Bangalore and were

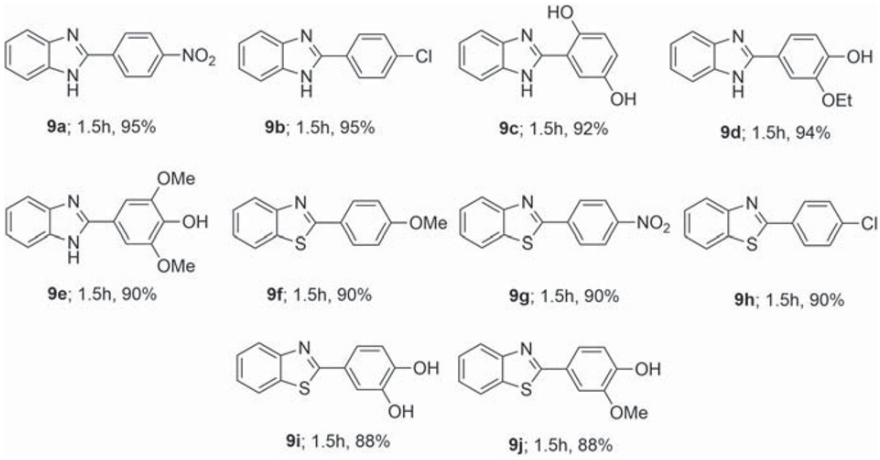

FIGURE 7 Synthesis of 2-arylbenzazole derivatives in the presence of MWCNTs-ZrO_2 nanocomposite

TABLE 3 Optimization of the reaction conditions for the synthesis of dihydroquinazolinone **12e**[a]

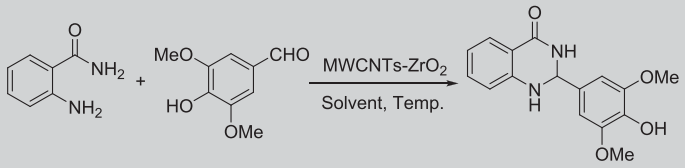

Entry	Solvent/catalyst	Temperature (°C)	Time (hr)	Yield (%)[b]
1	**H_2O/10 mg**	**r.t.**	**4**	**84**
2	H_2O/20 mg	r.t.	5	84
3	EtOH/10 mg	r.t.	4	80
4	MeOH/10 mg	r.t.	4	78
5	DCM/10 mg	r.t.	4	62
6	$CHCl_3$/10 mg	r.t.	4.5	56

Bold emphasis highlight the optimal reaction conditions giving excellent yield.
[a]Reaction conditions: 2-aminobenzamide (1 mmol), 4-hydroxy-3,5-dimethoxy benzaldehyde (1 mmol), and MWCNTs-ZrO_2 nanocomposite in solvent (5 ml).
[b]Isolated yield.

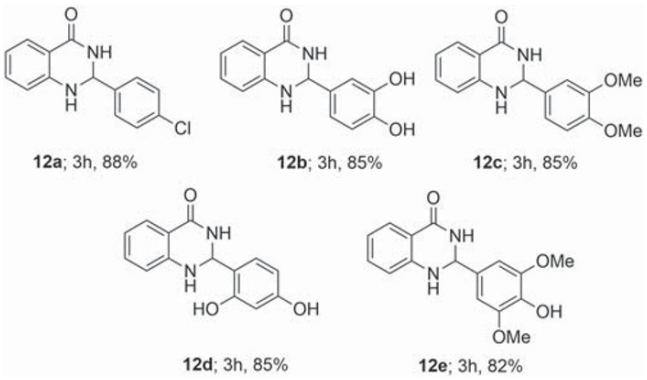

FIGURE 8 Synthesis of dihydroquinazolinone derivatives in the presence of MWCNTs-ZrO_2 nanocomposite

uncorrected. FT-IR spectra were recorded in the wavenumber range 4,000–400 cm^{-1} on a Perkin-Elmer, Bangalore FT-IR spectrometer RXI.

3.2 | Preparation of ZrO_2

A solution (30 ml) of 0.3 M $ZrO(NO_3)_2.H_2O$ using coconut juice as solvent was vigorously stirred followed by ultrasonication for 30 min. Subsequently, the solution was subjected to refluxing at 100°C for 24 hr. Finally, the white product was washed with distilled water until neutral pH was obtained, then it was dried in a vacuum oven at 60°C.

3.3 | Preparation of MWCNTs-ZrO_2 composite

MWCNTs were chemically oxidized by refluxing using concentrated HNO_3 and to form products referred to as MWCNT Ox.[58] Next, 2 wt% of oxidized MWCNTs was added to 30 ml of 0.3 M $ZrO(NO_3)_2.H_2O$ solution using coconut juice as solvent with vigorous stirring followed by its ultrasonication for 30 min. Subsequently, the whole dispersion was refluxed at 100°C for 24 hr. The black product obtained was washed with distilled water until neutral pH was reached followed by drying in a vacuum oven at 60°C. This product is MWCNTs-ZrO_2.

3.4 | General procedure for the synthesis of pyrazoles

A mixture of phenylhydrazine (**1**, 1 mmol), benzaldehyde (**2**, 1 mmol), manolonitrile (**3**, 1 mmol), and MWCNTs-ZrO_2 nanocomposite (10 mg) in 5 ml of water was stirred in a round-bottomed flask at room temperature for 1.5 hr. After completion of the reaction, the reaction mixture was extracted with ethyl acetate. The organic phase was dried over anhydrous Na_2SO_4 and removed under reduced pressure. Finally, the residue was washed with water and recrystallized from ethanol to afford the pure products **4a**–**p**. The products were characterized by FT-IR, ^1H and ^{13}C NMR spectroscopic analysis.

TABLE 4 Comparison of synthesis of products **4f** (entries 1–5), **7b** (entries 6–10), **9h** (entries 11–13), and **12b** (entries 14–17) with reported protocols

Sl no.	Compound	Catalyst	Condition	Yield (%)	Reference
1	**4f**	I_2	Water/r.t./6 min	92	[11]
2		PEG:H_2O	Ultrasonic irradiation/45 min	90	[13]
3		CuO/ZrO_2	Water/40°C/1.5 hr	89	[14]
4		Fe_3O_4@Si@MoO_2	Solvent-free/r.t./20 min	90	[16]
5		MWCNTs-ZrO_2	Water/r.t./1.5 hr	92	This work
6	**7b**	Ionic liquid-coated ZnO nanoparticles	Ball mill/r.t./22 min	95	[25]
7		Chitosan-supported Fe_3O_4	EtOH/r.t./4.5 hr	91	[26]
8		TFE	r.t./30 min	93	[28]
9		SDS micelles	Water/25°C/10 min	94	[29]
10		MWCNTs-ZrO_2	Water/r.t./3 hr	92	This work
11	**9h**	SDS micelles	Water/25°C/10 min	95	[29]
12		Bu^tONa	Toluene/100°C/24 hr	76	[33]
13		MWCNTs-ZrO_2	Water/r.t./1.5 hr	90	This work
14	**12b**	PEG-400	100–110°C	84	[35]
15		β-CD	Water/55–60°C	84	[37]
16		$[Ce(L\text{-}Pro)_2]_2$ (Oxa)	EtOH/50–55°C	81	[40]
17		MWCNTs-ZrO_2	Water/r.t./3 hr	85	This work

ButONa, Sodium tert-butoxide; CuO, Copper (II) oxide; EtOH, ethanol; Fe_3O_4, Iron oxide; H_2O = Water; I_2, Iodine; L-Pro, L-Proline; MoO_2, Molybdenum dioxide; MWCNTs-ZrO2, multi-walled carbonnanotubes-zirconia; Oxa, Oxalate; PEG, Polyethylene glycol; PEG-400, Polyethylene glycol-400; SDS, Sodium dodecyl sulfate; TFE, Trifluoroethanol; ZnO, Zinc oxide; ZrO_2, Zirconia; β-CD, beta-cyclodextrin.

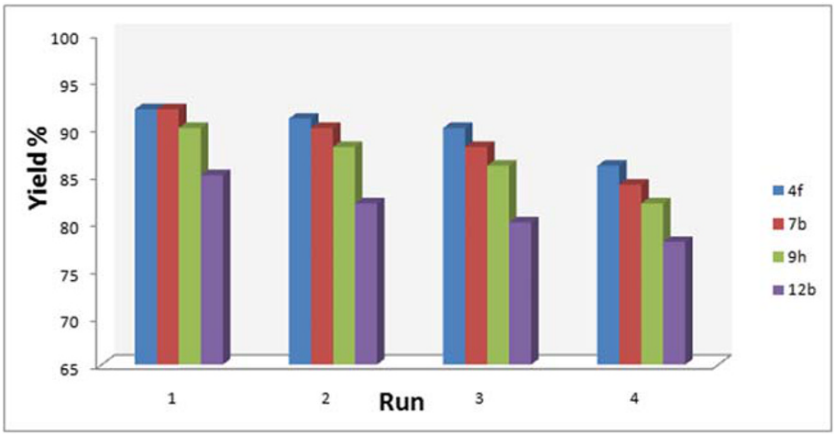

FIGURE 9 Reusability of MWCNTs-ZrO_2 for synthesis of **4f**, **7b**, **9h**, and **12b** products

3.5 | General procedure for the synthesis of 1,2-disubstituted benzimidazoles

A mixture of *o*-phenylenediamine (**5**, 1 mmol), benzaldehyde (**6**, 2 mmol), and MWCNTs-ZrO_2 (10 mg) in 5 ml of ethanol was stirred in a round-bottomed flask at room temperature for 3 hr. After completion of the reaction, the solvent was removed under reduced pressure and the residue was extracted with ethyl acetate and water. The ethyl acetate extract was dried over anhydrous Na_2SO_4 and removed under reduced pressure. Finally, the residue was washed with water and methanol to afford the pure products **7a**–**o**. The products were characterized by FT-IR, ^1H and ^{13}C NMR spectroscopic analysis.

3.6 | General procedure for the synthesis of 2-aryl benzimidazoles and 2-aryl benzothiazoles

A mixture of *o*-phenylenediamine (**5a**, 1 mmol), benzaldehyde (**8**, 1 mmol), and MWCNTs-ZrO_2 (10 mg) in 5 ml

of ethanol was stirred in a round-bottomed flask at room temperature for 2 hr. After completion of the reaction, an identical procedure (serial no. **3.5**) was adopted to get pure products **9a**–**e**. A similar procedure was used for reaction of *o*-aminothiophenol (**5b**, 1 mmol) and benzaldehyde (**8**, 1 mmol) in the presence of MWCNTs-ZrO_2 (10 mg) for the synthesis of 2-aryl benzothiazoles **9f**–**j**. The products were characterized by FT-IR, ^{1}H and ^{13}C NMR spectroscopic analysis.

3.7 | General procedure for the synthesis of dihydroquinazolinones

A mixture of anthranilamide (**10**, 1 mmol), benzaldehyde (**11**, 1 mmol), and MWCNTs-ZrO_2 (10 mg) in 5 ml of water was stirred in a round-bottomed flask at room temperature for 4 hr. After completion of the reaction, the reaction mixture was extracted with ethyl acetate. The organic phase was dried over anhydrous Na_2SO_4 and evaporated under reduced pressure. Finally, the residue was washed with water and recrystallized from ethanol to afford the pure products **12a**–**e**. The products were characterized by FT-IR, ^{1}H and ^{13}C NMR spectroscopic analysis.

3.8 | Spectral data for selected compounds

3.8.1 | 5-amino-3-(4-chlorophenyl)-1-phenyl-1*H*-pyrazole-4-carbonitrile (4b)

White solid, m.p. 130–132°C.[11] IR (KBr) υ_{max}: 3312, 3,035, 2,234, 1,679, 1,585, 1,490, 1,257, 1,089, 746 cm^{-1}. ^{1}H NMR (600 MHz, $CDCl_3$) δ: 7.64 (s, 2H), 7.60 (d, 2H, J = 8.3 Hz), 7.36 (d, 2H, J = 8.3 Hz), 7.32–7.28 (m, 2H), 7.13 (d, 2H, J = 7.9 Hz), 6.92 (t, 1H, J = 7.2 Hz) ppm. ^{13}C NMR (150 MHz, $CDCl_3$) δ: 158.3, 144.4, 135.9, 134.0, 133.9, 131.8, 130.1, 129.4, 128.8, 127.3, 120.4, 112.8 ppm.

3.8.2 | 5-amino-3-(4-hydroxy-3,5-dimethoxyphenyl)-1-phenyl-1*H*-pyrazole-4-carbonitrile (4o)

Orange oil. IR (KBr) υ_{max}: 3453, 2,932, 2,214, 1,592, 1,497, 1,453, 1,112 cm^{-1}. ^{1}H NMR (400 MHz, DMSO-d_6) δ: 10.10 (s, 1H), 8.55 (s, 1H), 7.73 (s, 1H), 7.18 (t, 2H, J = 7.4 Hz), 7.03 (d, 2H, J = 7.9 Hz), 6.89 (s, 2H), 6.69 (t, 1H, J = 7.2 Hz), 3.79 (s, 6H) ppm. ^{13}C NMR (100 MHz, DMSO-d_6) δ: 148.6, 146.0, 137.7, 136.6, 129.5, 126.7, 118.7, 112.3, 103.7, 56.4 ppm.

3.8.3 | 1-(4-methylbenzyl)-2-(*p*-tolyl)-1*H*-benzimidazole (7a)

White solid, m.p. 128–130°C.[28] IR (KBr) υ_{max}: 2941, 1,609, 1,516, 1,451, 748 cm^{-1}. ^{1}H NMR (400 MHz, $CDCl_3$) δ: 7.89 (d, 1H, J = 8.0 Hz), 7.61 (d, 2H, J = 7.9 Hz), 7.32–7.28 (m, 1H), 7.25 (d, 2H, J = 7.7 Hz), 7.20 (d, 2H, J = 5.7 Hz), 7.13 (d, 2H, J = 7.7 Hz), 6.99 (d, 2H, J = 7.7 Hz), 5.39 (s, 2H), 2.40 (s, 3H), 2.33 (s, 3H) ppm. ^{13}C NMR (100 MHz, $CDCl_3$) δ: 154.3, 143.2, 140.1, 137.4, 136.1, 133.5, 129.7, 129.5, 129.2, 127.2, 125.9, 122.9, 122.6, 119.8, 110.6, 48.2, 21.5, 21.1 ppm.

3.8.4 | 1-(4-hydroxy-3-chloro-benzyl)-2-(4-hydroxy-3-chloro-phenyl)-1H-benzimidazole (7j)

White solid, m.p. 232°C. IR (KBr) υ_{max}: 3407, 2,532, 1,600, 1,407, 745 cm^{-1}. ^{1}H NMR (600 MHz, DMSO-d_6) δ: 10.82 (s, 1H), 10.23 (s, 1H), 7.69 (s, 2H), 7.51 (dd, 2H, J = 12.8, 5.9 Hz), 7.25–7.24 (m, 2H), 7.11 (d, 1H, J = 8.4 Hz), 7.03 (s, 1H), 6.87 (d, 1H, J = 8.4 Hz), 6.74 (d, 1H, J = 8.4 Hz), 5.45 (s, 2H) ppm. ^{13}C NMR (150 MHz, DMSO-d_6) δ: 155.0, 152.9, 152.6, 143.0, 136.3, 131.0, 129.4, 129.1, 128.3, 126.4, 123.1, 122.7, 122.3, 120.5, 120.3, 119.6, 117.4, 117.2, 111.5, 47.0 ppm.

3.8.5 | 2-(4-hydroxy-3-ethoxyphenyl)-1*H*-benzimidazole (9d)

Chrome yellow solid, m.p. 108–110°C.[59] IR (KBr) υ_{max}: 3273, 2,914, 2,391, 1,587, 1,451, 1,265 cm^{-1}. ^{1}H NMR (600 MHz, DMSO-d_6) δ: 12.65 (bs, 1H), 9.48 (s, 1H), 7.74 (s, 1H), 7.62 (dd, 1H, J = 8.1, 1.1 Hz), 7.55 (s, 2H), 7.16 (dd, 2H, J = 5.5, 2.9 Hz), 6.94 (d, 1H, J = 8.2 Hz), 4.15 (q, 2H, J = 6.9 Hz), 1.40 (t, 3H, J = 6.9 Hz) ppm. ^{13}C NMR (150 MHz, DMSO-d_6) δ: 152.3, 149.2, 147.4, 122.1, 121.9, 120.1, 116.2, 112.0, 64.4, 15.2 ppm.

3.8.6 | 2-(4-nitrophenyl)-benzothiazole (9g)

Yellow solid, m.p. 230–232°C.[29] IR (KBr) υ_{max}: 3051, 1,630, 1,602, 1,502, 1,336, 763 cm^{-1}. ^{1}H NMR (500 MHz, $CDCl_3$) δ: 8.09 (d, 1H, J = 8.1 Hz), 8.06 (d, 2H, J = 8.4 Hz), 7.93 (d, 1H, J = 7.9 Hz), 7.54–7.49 (m, 3H), 7.43 (t, 1H, J = 7.6 Hz) ppm. ^{13}C NMR (125 MHz, $CDCl_3$) δ: 166.6, 154.1, 137.1, 135.1, 132.2, 129.3, 128.7, 126.5, 125.4, 123.3, 121.7 ppm.

3.8.7 | 2-(3,4-dihydroxyphenyl)-2,3-dihydroquinazolin-4(1*H*)-one (12b)

White solid, m.p. 291–293°C.[35] IR (KBr) υ_{max}: 3402, 3,244, 3,158, 1,645, 1,616, 1,508, 1,265 cm^{-1}. ^1H NMR (600 MHz, DMSO-d_6) δ: 9.02 (s, 1H), 8.98 (s, 1H), 8.07 (s, 1H), 7.61 (d, 1H, J = 6.6 Hz), 7.23 (d, 1H, J = 6.6 Hz), 6.92 (s, 2H), 6.724 (s,), 6.66 (d, 3H, J = 6 Hz), 5.58 (s, 1H) ppm. ^{13}C NMR (150 MHz, DMSO-d_6) δ: 164.2, 148.5, 146.1, 145.5, 133.7, 132.8, 127.8, 118.5, 117.4, 115.5, 115.3, 114.8, 114.7, 67.1 ppm.

4 | CONCLUSION

MWCNTs-ZrO_2 nanocomposite was successfully synthesized from the natural feedstock ACC, which acts as a green, environmentally friendly, and nontoxic solvent. Because of the acidic nature of ACC, it is the main source of protons and stimulates the formation of MWCNTs-ZrO_2. The nanocomposite was characterized by FT-IR, XRD, FE-SEM, and XPS analysis. It is noteworthy that the synthesized nanocomposite was used as a heterogeneous and reusable nanocatalyst in the field of organic synthesis for the first time. Various *N*-heterocyclic compounds such as pyrazoles, disubstituted benzimidazoles, 2-arylbenzazoles, and dihydroquinazolinones were synthesized using the MWCNTs-ZrO_2 nanocomposite under ecofriendly reaction conditions. The major advantages of the protocol are short reaction time, good to excellent yield, green reaction conditions, and recyclability without significant loss in catalytic activity, and these factors open up a new horizon in organic synthesis.

ACKNOWLEDGMENTS

We thank University Grants Commission, New Delhi for financial support of this work [Ref No.- 21/06/2015(i)EU-V].

ORCID

Bipasa Halder https://orcid.org/0000-0002-0138-9084
Flora Banerjee https://orcid.org/0000-0003-3257-8942
Ahindra Nag https://orcid.org/0000-0001-5924-8981

REFERENCES

[1] a) Z.-Y. Mao, X.-Y. Liao, H.-S. Wang, C.-G. Wang, K.-B. Huang, Y.-M. Pan, *RSC Adv.* **2017**, *7*, 13123. b) A. Kumar, D. Saxena, M. K. Gupta, *Green Chem.* **2013**, *15*, 2699. c) A. P. Rajput, A. R. Kankhare, *Int. J. Pharm. Sci. Invent.* **2017**, *6*, 19.
[2] R. Sridhar, P. T. Perumal, S. Etti, G. Shanmugam, M. N. Ponnuswamy, V. R. Prabavathy, N. Mathivanan, *Bioorg. Med. Chem. Lett.* **2004**, *14*, 6035.
[3] A. A. Bekhit, H. T. Y. Fahmy, S. A. F. Rostom, A. M. Baraka, *Eur. J. Med. Chem.* **2003**, *38*, 27.
[4] O. I. El-Sabbagh, M. M. Baraka, S. M. Ibrahim, C. Pannecouque, G. Andrei, R. Snoeck, J. Balzarini, A. A. Rashad, *Eur. J. Med. Chem.* **2009**, *44*, 3746.
[5] G. R. Bebernitz, G. Argentieri, B. Battle, C. Brennan, B. Balkan, B. F. Burkey, M. Eckhardt, J. Gao, P. Kapa, R. J. Strohschein, H. F. Schuster, M. Wilson, D. D. Xu, *J. Med. Chem.* **2001**, *44*, 2601.
[6] S. Manfredini, R. Bazzanini, P. G. Baraldi, M. Bonora, M. Marangoni, D. Simoni, A. Pani, F. Scintu, E. Pinna, L. Pisano, P. La Colla, *Anti-Cancer Drug des.* **1996**, *11*, 193.
[7] S. G. Alegaon, K. R. Alagawadi, M. K. Garg, K. Dushyant, D. Vinod, *Bioorg. Chem.* **2014**, *54*, 51.
[8] G. Menozzi, L. Mosti, P. Fossa, F. Mattioli, M. Ghia, *J. Heterocycl. Chem.* **1997**, *34*, 963.
[9] D. M. Bailey, P. E. Hansen, A. G. Hlavac, E. R. Baizman, J. Pearl, A. F. DeFelice, M. E. Feigenson, *J. Med. Chem.* **1985**, *28*, 256.
[10] Z. Özdemir, H. B. Kandilci, B. Gümüşel, U. Çalış, A. A. Bilgin, *Eur. J. Med. Chem.* **2007**, *42*, 373.
[11] xM. Srivastava, P. Rai, J. Singh, J. Singh, *New J. Chem.* **2014**, *38*, 302.
[12] S. Kumari, A. Shekhar, D. D. Pathak, *New J. Chem.* **2016**, *40*, 5053.
[13] F. Nemati, S. H. Nikkhah, A. Elhampour, *Chin. Chem. Lett.* **2015**, *26*, 1397.
[14] S. Maddila, S. Rana, R. Pagadala, S. Kankala, S. Maddila, S. B. Jonnalagadda, *Catal. Commun.* **2015**, *61*, 26.
[15] M. A. Zolfigol, F. Afsharnadery, S. Baghery, S. Salehzadeh, F. Maleki, *RSC Adv.* **2015**, *5*, 75555.
[16] J. Rakhtshah, S. Salehzadeh, E. Gowdini, F. Maleki, S. Baghery, M. A. Zolfigol, *RSC Adv.* **2016**, *6*, 104875.
[17] P. Arora, J. K. Rajput, *J. Mater. Sci.* **2017**, *52*, 11413.
[18] E. S. Lazer, M. R. Matteo, G. J. Possanza, *J. Med. Chem.* **1987**, *30*, 726.
[19] G. Navarette-Vázquez, R. Cedillo, A. Hernández-Campos, A. Yépez, F. Hernández-Luis, J. Valdez, R. Morales, R. Cortés, M. Hernández, R. Castillo, *Bioorg. Med. Chem. Lett.* **2001**, *11*, 187.
[20] A. T. Mavrova, P. Denkova, Y. A. Tsenov, K. K. Anichina, D. I. Vutchev, *Bioorg. Med. Chem.* **2007**, *15*, 6291.
[21] N. S. Pawar, D. S. Dalal, S. R. Shimpi, P. P. Mahulikar, *Eur. J. Pharm. Sci.* **2004**, *21*, 115.
[22] K. Starčević, M. Kralj, K. Ester, I. Sabol, M. Grce, K. Pavelić, G. Karminski-Zamola, *Bioorg. Med. Chem.* **2007**, *15*, 4419.
[23] H. Zarrinmayerh, D. M. Zimmerman, B. E. Cantrell, D. A. Schober, R. F. Bruns, S. L. Gackenheimer, P. L. Orustein, P. A. Hipskind, T. C. Britton, D. R. Gehlert, *Bioorg. Med. Chem. Lett.* **1999**, *9*, 647.
[24] R. K. Jat, J. L. Jat, D. P. Pathak, *E-J. Chem.* **2006**, *3*, 278.
[25] H. Sharma, N. Kaur, N. Singh, D. O. Jang, *Green Chem.* **2015**, *17*, 4263.
[26] A. Maleki, N. Ghamari, M. Kamalzare, *RSC Adv.* **2014**, *4*, 9416.
[27] V. Ravi, E. Ramu, K. Vijay, A. S. Rao, *Chem. Pharm. Bull.* **2007**, *55*, 1254.
[28] R. Chebolu, D. N. Kommi, D. Kumar, N. Bollineni, A. K. Chakraborti, *J. Org. Chem.* **2012**, *77*, 10158.
[29] K. Bahrami, M. M. Khodaei, A. Nejati, *Green Chem.* **2010**, *12*, 1237.

[30] N. H. Cano, J. G. Uranga, M. Nardi, A. Procopio, D. A. Wunderlin, A. N. Santiago, *Beilstein J. Org. Chem.* **2016**, *12*, 2410.
[31] M. Karthik, P. Suresh, *New J. Chem.* **2018**, *42*, 17931.
[32] D. Kommula, S. R. M. Madugula, *J. Iran. Chem. Soc.* **2017**, *14*, 1665.
[33] X. Shi, J. Guo, J. Liu, M. Ye, Q. Xu, *Chem. – Eur. J.* **2015**, *21*, 9988.
[34] S. Sharma, D. Bhattacherjee, P. Das, *Org. Biomol. Chem.* **2018**, *16*, 1337.
[35] P. Yerram, R. Chowrasia, S. Seeka, S. J. Tangenda, *Eur. J. Chem.* **2013**, *4*, 462.
[36] M. Dabiri, P. Salehi, M. Baghbanzadeh, M. A. Zolfigol, M. Agheb, S. Heydari, *Catal. Commun.* **2008**, *9*, 785.
[37] K. Ramesh, K. Karnakar, G. Satish, B. S. P. A. Kumar, Y. V. D. Nageswar, *Tetrahedron Lett.* **2012**, *53*, 6936.
[38] J. Safari, S. Gandomi-Ravandi, *C. R. Chim.* **2013**, *16*, 1158.
[39] P. Salehi, M. Dabiri, M. Baghbanzadeh, M. Bahramnejad, *Synth. Commun.* **2006**, *36*, 2287.
[40] R. Katla, R. Chowrasia, C. D. G. da Silva, A. R. de Oliveira, B. F. dos Santos, N. L. C. Domingues, *Synthesis* **2017**, *49*, 5143.
[41] a) A. Baiker, *Chem. Rev.* **1999**, *99*, 453. b) S.-H. Lee, S. T. Kadam, *Appl. Organomet. Chem.* **2011**, *25*, 608. c) A. Corma, H. García, F. X. L. Xamena, *Chem. Rev.* **2010**, *110*, 4606. d) Z. Guo, B. Liu, Q. Zhang, W. Deng, Y. Wang, Y. Yang, *Chem. Soc. Rev.* **2014**, *43*, 3480. e) M. Rohaniyan, A. Davoodnia, A. Nakhaei, *Appl. Organomet. Chem.* **2016**, *30*, 626.
[42] a) G. I. Shakibaei, P. Mirzaei, A. Bazgir, *Appl. Catal. A: Gen.* **2007**, *325*, 188. b) H. Veisi, M. R. P. Heravi, M. Hamelian, *Appl. Organomet. Chem.* **2015**, *29*, 334.
[43] M. Melchionna, S. Marchesan, M. Prato, P. Fornasiero, *Catal. Sci. Technol.* **2015**, *5*, 3859.
[44] G. G. Wildgoose, C. E. Banks, R. G. Compton, *Small* **2006**, *2*, 182.
[45] a) J. Safari, S. Gandomi-Ravandi, *J. Mol. Catal. A: Chem.* **2014**, *390*, 1. b) H. He, L. A. Pham-Huy, P. Dramou, D. Xiao, P. Zuo, C. Pham-Huy, *BioMed Res. Int.* **2013**, *2013*, 578290.
[46] a) K. Tanabe, *Mater. Chem. Phys.* **1985**, *13*, 347. b) G. D. Wilk, R. M. Wallace, J. M. Anthony, *J. Appl. Phys.* **2001**, *89*, 5243. c) R. C. Garvie, R. H. Hannink, R. T. Pascoe, *Nature* **1975**, *258*, 703.
[47] a) A. H. Heuer, L. W. Hobbs, *Sci. Technol. Zirconia am. Ceramic Soc. Columbus Ohio* **1981**, *3*, 241. b) A. Krell, J. Klimke, T. Hutzler, *Opt. Mater.* **2009**, *31*, 1144. c) J. Robertson, *Rep. Prog. Phys.* **2006**, *69*, 327. d) G. Liu, Y. Lin, *Anal. Chem.* **2005**, *77*, 5894. e) M. Inoue, H. Kominami, T. Inui, *Appl. Catal. A: Gen.* **1993**, *97*, L25. f) J. Joo, T. Yu, Y. W. Kim, H. M. Park, F. Wu, J. Z. Zhang, T. Hyeon, *J. Am. Chem. Soc.* **2003**, *125*, 6553. g) R. C. Buchanan, S. Pope, *J. Electrochem. Soc.* **1983**, *130*, 962. h) X. Luo, A. Morrin, A. J. Killard, M. R. Smyth, *Electroanalysis* **2006**, *18*, 319. i) S. A. Steiner, T. F. Baumann, B. C. Bayer, R. Blume, M. A. Worsley, W. J. MoberlyChan, E. L. Shaw, R. Schlögl, A. J. Hart, S. Hofmann, B. L. Wardle, *J. Am. Chem. Soc.* **2009**, *131*, 12144. j) J. Lu, J. B. Zang, S. X. Shan, H. Huang, Y. H. Wang, *Nano Lett.* **2008**, *8*, 4070. k) T. Z. Sholklapper, V. Radmilovic, C. P. Jacobson, S. J. Visco, L. C. De Jonghe, *Electrochem. Solid-State Lett.* **2007**, *10*, B74.
[48] K. Ghosh, S. K. Srivastava, S. Puravankara, *J. Nanosci. Nanotechnol.* **2019**, *19*, 3367.
[49] a) E. Kolvari, M. A. Zolfigol, H. Banary, *Chin. Chem. Lett.* **2011**, *22*, 1305. b) B. Maleki, N. Nasiri, R. Tayebee, A. Khojastehnezhad, H. A. Akhlaghi, *RSC Adv.* **2016**, *6*, 79128..
[50] Selected references:a) R. Pal, *Int. J. Adv. Chem.* **2014**, *2*, 27. b) S. D. Bagul, J. D. Rajput, R. S. Bendre, *Environ. Chem. Lett.* **2017**, *15*, 725. c) H. V. Chavan, B. P. Bandgar, *ACS Sustainable Chem. Eng.* **2013**, *1*, 929. d) G. Kumaraswamy, S. Ramesh, *Green Chem.* **2003**, *5*, 306. e) A. N. Geraldes, A. A. da Silva, J. Leal, G. M. Estrada-Villegas, N. Lincopan, K. V. Katti, A. B. Lugão, *Adv. Nanoparticles* **2016**, *5*, 176. f) E. K. Elumalai, K. Kayalvizhi, S. Silvan, *J. Pharm. Bioall. Sci.* **2014**, *6*, 241. g) S. Naghdi, M. Sajjadi, M. Nasrollahzadeh, K. Y. Rhee, S. M. Sajadi, B. Jaleh, *J. Taiwan Inst. Chem. E.* **2018**, *86*, 158.
[51] a) A. Prades, M. Dornier, N. Diop, J.-P. Pain, *Fruits* **2012**, *67*, 157. b) J. W. H. Yong, L. Ge, Y. F. Ng, S. N. Tan, *Molecules* **2009**, *14*, 5144. c) K. Misra, H. S. Maity, S. Chanda, A. Nag, *J. Mol. Catal. B: Enzym.* **2012**, *82*, 92.
[52] A. Nikam, T. Pagar, S. Ghotekar, K. Pagar, S. Pansambal, *J. Chem. Rev.* **2019**, *1*, 154.
[53] a) L. Stobinski, B. Lesiak, L. Kövér, J. Tóth, S. Biniak, G. Trykowski, J. Judek, *J. Alloys Compd.* **2010**, *501*, 77. b) H. Fayazfar, A. Afshar, A. Dolati, *Mater. Sci. Appl.* **2013**, *4*, 667. c) H. M. Altass, A. E. R. S. Khder, *J. Mol. Catal. A: Chem.* **2016**, *411*, 138. d) E. F. Lopez, V. S. Escribano, M. Panizza, M. M. Carnasciali, G. Busca, *J. Mater. Chem.* **2001**, *11*, 1891.
[54] S. Giri, D. Ghosh, C. K. Das, *Adv. Funct. Mater.* **2014**, *24*, 1312.
[55] a) S. Sankal, C. Kaynak, *J. Reinf. Plast. Compos.* **2013**, *32*, 75. b) A. S. K. Kumar, S.-J. Jiang, W.-L. Tseng, *J. Mater. Chem. A* **2015**, *3*, 7044.
[56] a) P. Su, X. Ji, C. Liu, W. Gao, R. Fu, C. Tang, B. Cheng, *RSC Adv.* **2015**, *5*, 36467. b) G. Wang, L. Chen, Y. Sun, J. Wu, M. Fu, D. Ye, *RSC Adv.* **2015**, *5*, 45320.
[57] a) P. K. Gupta, S. Tiwari, Z. H. Khan, P. R. Solanki, *J. Mater. Chem. B* **2017**, *5*, 2019. b) J. Zhou, X. Zha, F. Y. Chen, Q. Ye, P. Eklund, S. Du, Q. Huang, *Angew. Chem. Int. Ed.* **2016**, *55*, 5008.
[58] I. D. Rosca, F. Watari, M. Uo, T. Akasaka, *Carbon* **2005**, *43*, 3124.
[59] E. A. Dikusar, V. I. Potkin, *Russ. J. Org. Chem.* **2010**, *46*, 268.

Note. r.t., room temperature.
Note. r.t., room temperature.
Note. r.t., room temperature.

SUPPORTING INFORMATION

Additional supporting information may be found online in the Supporting Information section at the end of this article.

How to cite this article: Halder B, Banerjee F, Nag A. MWCNTs-ZrO_2 as a reusable heterogeneous catalyst for the synthesis of *N*-heterocyclic scaffolds under green reaction medium. *Appl Organomet Chem*. 2020;e5906. https://doi.org/10.1002/aoc.5906